

Entropy-based Discovery of Summary Causal Graphs in Time Series

Karim Assaad^{1,2}, Emilie Devijver¹, Eric Gaussier¹, and Ali Aït-Bachir²

¹Univ. Grenoble Alpes, CNRS, Grenoble INP, LIG
²Coservit

May 24, 2021

Abstract

We address in this study the problem of learning a summary causal graph on time series with potentially different sampling rates. To do so, we first propose a new temporal mutual information measure defined on a window-based representation of time series. We then show how this measure relates to an entropy reduction principle that can be seen as a special case of the Probabilistic Raising Principle. We finally combine these two ingredients in a PC-like algorithm to construct the summary causal graph. This algorithm is evaluated on several datasets that shows both its efficacy and efficiency.

1 Introduction

Time series arise as soon as observations, from sensors or experiments, for example, are collected over time. They are present in various forms in many different domains, as healthcare (through, *e.g.*, monitoring systems), Industry 4.0 (through, *e.g.*, predictive maintenance and industrial monitoring systems), surveillance systems (from images, acoustic signals, seismic waves, etc.) or energy management (through, *e.g.* energy consumption data) to name but a few. We are interested in this study in analyzing time series to detect the causal relations that exist between them. We focus in particular on the summary graph, as opposed to the full time graph, as it provides a simple and efficient view on the causal relations that exist between time series. Figure 1 illustrates the difference between a full time graph (left) and a summary graph (middle and right). The representation on the right emphasizes the fact that the causal graph is acyclic.

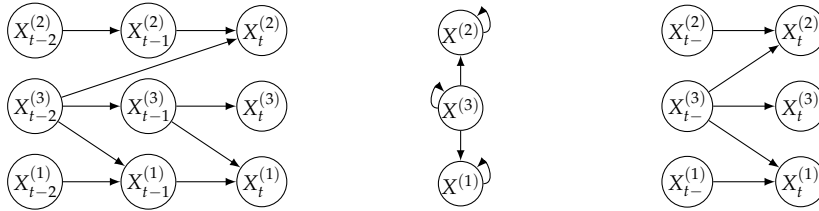


Figure 1: Example of a full time causal graph (left) and a summary causal graph (middle and right).

An important aspect of real-world time series is that different time series, as they measure different elements, usually have different sampling rates. Despite this, the algorithms that have been developed so far to discover causal structures from temporal observations [Granger, 1969, Hyvärinen et al., 2010, Moneta et al., 2013, Peters et al., 2013, Runge et al., 2019, Nauta et al., 2019] rely on the idealized assumptions that all time series have the same sampling rates with identical timestamps¹. We introduce in this paper a causal inference algorithm that can be applied to discrete time series with continuous values and different sampling rates. The skeleton construction (as well as the orientation of instantaneous relations) is similar to PC algorithm [Spirtes et al., 2000], but adapted to time series. For orienting lagged relations, it calls upon an entropic reduction principle which is inspired by the work of Suppes [1970]. The algorithm we propose can be used in situations where all common causes are observed. At its core lies (in)dependence measures, to detect relevant dependencies, which are based here on an information theoretic approach. Indeed, information measures are particularly interesting due to their non parametric nature, their robustness against strictly monotonic transformations, which makes them capable of handling nonlinear distortions in the system, and their good behavior in previous studies on causal discovery [Affeldt and Isambert, 2015].

Our contributions are four-fold. First of all, we show that directly addressing the problem of learning summary causal graphs, without first resorting to full time graphs, can be beneficial. To do so, we propose a new temporal mutual information measure defined on a window-based representation of time series. We then show how this measure relates to an entropy reduction principle which can be seen as a special case of the Probabilistic Raising Principle. We finally combine these two ingredients in a PC-like algorithm to construct the summary causal graph. Our evaluation, conducted on several datasets, illustrates the efficacy and efficiency of our approach.

The remainder of the paper is organized as follows: Section 2 describes related work. Section 3 then introduces the (conditional) mutual information

¹Assuming identical timestamps in the case of identical sampling rates seems reasonable as one can shift time series so that they coincide in time.

measures we propose for time series and the entropy reduction principle that our method is based on. Section 4 presents the causal discovery algorithm we have developed on top of these measures. The causal discovery algorithm we propose is illustrated and evaluated on 5 different datasets, including time series with equal and different sampling rates and a real dataset, in Section 5. Finally, Section 6 concludes the paper.

2 Related Work

Granger Causality is one of the oldest methods proposed to detect causal relations between time series. However, in its standard form [Granger, 1969], it is known to handle a restricted version of causality that focuses on causal priorities as it assumes that the past of a cause is necessary and sufficient for optimally forecasting its effect. This approach has nevertheless been improved since then [Granger, 2004], and has recently been explored through an attention mechanism within convolutional networks [Nauta et al., 2019].

In a different line, approaches based on Structural Equation Models assume that the causal system can be defined by a set of equations that explain each variable by its direct causes and an additional noise. Causal relations are in this case discovered using footprints produced by the causal asymmetry in the data. For time series, the most popular algorithms in this family are tsLiNGAM [Hyvärinen et al., 2008], which is an extension of LiNGAM through autoregressive models, and TiMINo [Peters et al., 2013], which discovers a causal relationship by looking at independence between the noise and the potential causes. The main drawbacks of these approaches are the need of a large sample size to achieve good performance and the simplifying assumptions they make on the relations between causes and effects [Malinsky and Danks, 2018].

Nowadays, the most popular approaches for inferring causal graphs are certainly constraint-based approaches, based on the PC algorithm by Spirtes et al. [2000]. Several algorithms, adapted from non-temporal causal graph discovery algorithms, have been proposed in this family for time series, from ANLTSM by Chu and Glymour [2008] to PCMCI by Runge et al. [2019]. Other variants such as tsFCI by Entner and Hoyer [2010] and SVAR-FCI by Malinsky and Spirtes [2018] focus on hidden causes, a case we do not consider here. Our work is thus more closely related to that of Runge et al. [2019]. However, we focus here on the summary causal graph, whereas PCMCI produces a full temporal graph, and introduce a new temporal mutual information measure and entropy reduction principle on which we ground our PC-like algorithm.

Since their introduction [Shannon, 1948], information theoretic measures have become very popular. However, their application to temporal data raises several problems related to the fact that time series may have different sampling rates, can be shifted in time and may have strong internal dependencies. Many studies have attempted to re-formalize mutual information for time series: Galka et al. [2006] decorrelated observations by whitening data (which may have severe consequences on causal relations); Schreiber [2000]

represents the information flow from one state to another within the transfer entropy, which is thus asymmetric; Frenzel and Pompe [2007], inspired by Kraskov et al. [2004], represented time series by vectors that are assumed to be statistically independent; the Time Delayed Mutual Information proposed in Albers and Hripcsak [2012], closer to our proposal², aims at addressing the problem of non uniform sampling rates. The measure we propose is more suited to discover summary graph as it can consider potentially complex relations between timestamps in different time series through the use of window-based representations and compatible time lags, and is more general as it can consider different sampling rate.

3 Information measures for causal discovery in Time Series

We present in this section a new mutual information measures that operate on a window-based representation of time series to assess whether time series are (conditionally) dependent or not. We then show how this measure is related to an Entropy Reduction Principle that is a special case of the Probabilistic Raising Principle [Suppes, 1970].

We first assume that all time series are aligned in time, with the same sampling rate, prior to show how our development can be applied to time series with different sampling rates. Without loss of generality, time instants are assumed to be integers. Lastly, as done in previous studies [Schreiber, 2000], we assume that all time series are first-order Markov self-causal (any time instant is caused by its previous instant within the same time series).

3.1 Causal temporal mutual information

Let us consider d univariate time series $X^{(1)}, \dots, X^{(d)}$, and their observations $(v_1^{(p)}, \dots, v_{L_p}^{(p)})$ ($1 \leq p \leq d$), where $v_t^{(p)}$ ($1 \leq t \leq L_p$) is the value for the p -th time series at time index t and L_p is the length of $X^{(p)}$. Throughout this section, we will make use of the following example, illustrated in Figure 2, to discuss the notions we introduce.

Example 1. *Let us consider the following two time series defined by, for all t ,*

$$\begin{aligned} X_t^{(p)} &= X_{t-1}^{(p)} + \eta_t^{(p)}, \\ X_t^{(q)} &= X_{t-1}^{(q)} + X_{t-2}^{(p)} + X_{t-1}^{(p)} + \eta_t^{(q)}, \end{aligned}$$

with $(\eta_t^{(p)}, \eta_t^{(q)}) \sim \mathcal{N}(0, 1)$.

²It can be seen as a special case of our measure by considering windows of size 1 and a single time series.

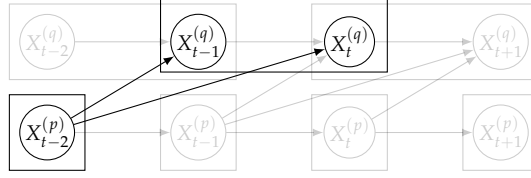


Figure 2: Why do we need windows and lags? An illustration with two time series where $X^{(p)}$ causes $X^{(q)}$ in two steps (circles correspond to observed points and rectangles to windows). The arrows in black are discussed in the text.

One can see in Example 1 that, in order to capture the dependencies between the two time series, one needs to take into account a lag between them, as the true, causal relations are not instantaneous. Several studies have recognized the importance of taking into account lags to measure (conditional) dependencies between time series; for example, Runge et al. [2019] uses point-wise mutual information between time series with lags to assess whether they are dependent or not.

In addition to lags, Example 1 also reveals that a window-based representation may be necessary to fully capture the dependencies between the two time series. Indeed, as $X_{t-1}^{(q)}$ and $X_t^{(q)}$ are the effects of the same cause ($X_{t-2}^{(p)}$), it may be convenient to consider them together when assessing whether the time series are dependent or not. For example, defining (overlapping) windows of size two for $X^{(q)}$ and one for $X^{(p)}$ with a lag of 1 from $X^{(p)}$ to $X^{(q)}$, as in Figure 2, allows one to fully represent the causal dependencies between the two time series.

Definition 1. Let $X^{(p)}$ and $X^{(q)}$ be two time series. The window-based representation, of size $0 < \lambda_{pq} < L_p$, of the time series $X^{(p)}$ wrt $X^{(q)}$, which will be denoted $X^{(p;\lambda_{pq})}$, simply amounts to considering $(L_p - \lambda_{pq} + 1)$ windows: $w_t^{(p;\lambda_{pq})} = (v_t^{(p)}, \dots, v_{t+\lambda_{pq}-1}^{(p)})$, $1 \leq t \leq L_p - \lambda_{pq} + 1$. The window-based representation, of size $0 < \lambda_{qp} < L_q$, of the time series $X^{(q)}$ wrt $X^{(p)}$ is defined in the same way. A temporal gap $\gamma_{pq} \in \mathbb{Z}$ compatible with λ_{pq} and λ_{qp} relates windows in $X^{(p;\lambda_{pq})}$ and $X^{(q;\lambda_{qp})}$ in such a way that the starting time of the related windows are separated by γ_{pq} . We denote by $\mathcal{C}^{(p,q)}$ the set of window sizes and compatible temporal lags.

Based on the above elements, we define the *causal temporal mutual information* between two time series as the maximum of the standard mutual information over all possible compatible temporal lags and windows, conditioned by the past of the two series. Indeed, as we are interested in obtaining a summary graph, we don't have to consider all the potential dependencies between two time series (which would be necessary for inferring a temporal graph). Using the maximum over all possible associations is a way to summarize all temporal dependencies which ensures that one does not miss a dependency between the

two time series. Furthermore, conditioning on the past allows one to eliminate spurious dependencies in the form of auto-correlation, as in transfer entropy [Schreiber, 2000]. We follow this idea here and, as in transfer entropy, consider windows of size 1 and a temporal lag of 1 for conditioning on the past, which is in line with the first-order Markov self-causal assumption mentioned above.

Definition 2. Consider two time series $X^{(p)}$ and $X^{(q)}$. We define the causal temporal mutual information between $X^{(p)}$ and $X^{(q)}$ as:

$$\begin{aligned} \text{CTMI}(X^{(p)}; X^{(q)}) = & \max_{(\lambda_{pq}, \lambda_{qp}, \gamma_{pq}) \in \mathcal{C}^{(p,q)}} I(X_t^{(p; \lambda_{pq})}; X_{t+\gamma_{pq}}^{(q; \lambda_{qp})} | X_{t-1}^{(p; 1)}, X_{t+\gamma_{pq}-1}^{(q; 1)}) \\ & \triangleq I(X_t^{(p; \bar{\lambda}_{pq})}; X_{t+\bar{\gamma}_{pq}}^{(q; \bar{\lambda}_{qp})} | X_{t-1}^{(p; 1)}, X_{t+\bar{\gamma}_{pq}-1}^{(q; 1)}), \end{aligned} \quad (1)$$

where I represents the mutual information and $\bar{\gamma}_{pq}$, $\bar{\lambda}_{pq}$, and $\bar{\lambda}_{qp}$ resp. correspond to the optimal lag and optimal windows.

In the context we have retained, in which dependencies are constant over time, CTMI satisfies standard properties of mutual information, namely it is nonnegative, symmetric and equals to 0 iff time series are independent. Thus, two time series $X^{(p)}$ and $X^{(q)}$ such that $\text{CTMI}(X^{(p)}; X^{(q)}) > 0$ are dependent.

Example 1, continuation. The optimal window size $\bar{\lambda}_{pq}$ is equal to 1 as $X^{(p)}$ has no other cause than itself; $\bar{\lambda}_{qp}$ is equal to 2 as $X^{(p)}$ causes only (except itself) $X_{t+1}^{(q)}$ and $X_t^{(q)}$. Furthermore, $\bar{\gamma}_{pq} = 1$ and $\text{CTMI}(X^{(p)}; X^{(q)}) = \log(3)/2$, whereas the standard mutual information (conditioned on the past, with no lags and windows) is equal to 0.

3.2 Entropy reduction principle

Interestingly, CTMI can be related to a version of the Probabilistic Raising Principle (PRP, Suppes [1970]) that states that a cause, here a time series, raises the probability of any of its effects, here another time series, even when the past of the two time series is taken into account, meaning that the relation between the two time series is not negligible compared to the internal dependencies of the time series. In this context, the following definition generalizes to window-based representations of time series the standard definition of *prima facie* causes for discrete variables.

Definition 3 (Prima facie cause). Let $X^{(p)}$ and $X^{(q)}$ be two time series with window sizes λ_{pq} and λ_{qp} and let $P_{t,t'} = (X_{t-1}^{(p; 1)}, X_{t'-1}^{(q; 1)})$ represent the past of $X^{(p)}$ and $X^{(q)}$ for any two instants (t, t') . We say that $X^{(p)}$ is a *prima facie* cause of $X^{(q)}$ with delay $\gamma_{pq} > 0$ iff there exist Borel sets B_p , B_q and B_P such that one has:

$$\begin{aligned} P(X_{t+\gamma_{pq}}^{(q; \lambda_{qp})} \in B_q | X_t^{(p; \lambda_{pq})} \in B_p, P_{t, t+\gamma_{pq}} \in B_P) &> \\ P(X_{t+\gamma_{pq}}^{(q; \lambda_{qp})} \in B_q | P_{t, t+\gamma_{pq}} \in B_P). \end{aligned}$$

We now introduce a slightly different principle based on the causal temporal mutual information which we refer to as the *entropy reduction principle* (ERP).

Definition 4 (Entropic prima facie cause). *Using the same notations as in Def. 3, we say that $X^{(p)}$ is an entropic prima facie cause of $X^{(q)}$ with delay $\gamma_{pq} > 0$ iff $I(X_t^{(p;\lambda_{pq})}; X_{t+\gamma_{pq}}^{(q;\lambda_{qp})} | P_{t,t+\gamma_{pq}}) > 0$.*

Note that considering that the above mutual information is positive is equivalent to considering that the entropy of $X^{(q)}$ when conditioned on the past reduces when one further conditions on $X^{(p)}$. One has the following relation between the ERP and PRP principles.

Property 1. *With the same notations, if $X^{(p)}$ is an entropic prima facie cause of $X^{(q)}$ with delay $\gamma_{pq} > 0$, then $X^{(p)}$ is a prima facie cause of $X^{(q)}$ with delay $\gamma_{pq} > 0$. Furthermore, if $\text{CTMI}(X^{(p)}; X^{(q)}) > 0$ with $\tilde{\gamma}_{pq} > 0$ then $X^{(p)}$ is an entropic prima facie cause of $X^{(q)}$ with delay $\tilde{\gamma}_{pq}$.*

Proof. Let us assume that $X^{(p)}$ is not a *prima facie* cause of $X^{(q)}$ for the delay γ_{pq} . Then, for all Borel sets B_p, B_q and B_P one has $P(X_{t+\gamma_{pq}}^{(q;\lambda_{qp})} \in B_q | X_t^{(p;\lambda_{pq})} \in B_p, P_{t,t+\gamma_{pq}} \in B_P) \leq P(X_{t+\gamma_{pq}}^{(q;\lambda_{qp})} \in B_q | P_{t,t+\gamma_{pq}} \in B_P)$. This translates, in terms of density functions denoted f , as: $\forall (x_t^{(p)}, x_{t+\gamma_{pq}}^{(q)}, p_{t,t+\gamma_{pq}}), f(x_{t+\gamma_{pq}}^{(q)} | x_t^{(p)}, p_{t,t+\gamma_{pq}}) \leq f(x_{t+\gamma_{pq}}^{(q)} | p_{t,t+\gamma_{pq}})$, which implies that $H(X_{t+\gamma_{pq}}^{(q;\lambda_{qp})} \in B_q | X_t^{(p;\lambda_{pq})} \in B_p, P_{t,t+\gamma_{pq}} \in B_P)$ is greater than $H(X_{t+\gamma_{pq}}^{(q;\lambda_{qp})} \in B_q | P_{t,t+\gamma_{pq}} \in B_P)$ so that $X^{(p)}$ is not an *entropic prima facie* cause of $X^{(q)}$ with delay γ_{pq} . By contraposition, we conclude the proof of the first statement. The second statement directly derives from the definition of CTMI. \square

3.3 Conditional causal temporal mutual information

We now extend the causal temporal mutual information by conditioning on a set of variables. In a causal discovery setting, conditioning is used to assess whether two dependent time series can be made independent by conditioning on connected time series, *i.e.* time series which are dependent with at least one of the two times series under consideration. Figure 3 illustrates the case where the dependence between $X^{(p)}$ and $X^{(q)}$ is due to spurious correlations originating from common causes. Conditioning on these common causes should lead to conditional independence of the two time series. Of course, the conditional variables should precede in time the two time series under consideration. This leads us to the following definition of the conditional causal temporal mutual information.

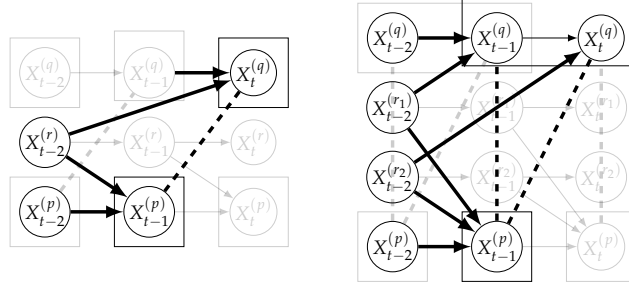


Figure 3: Examples of conditional independence between dependent time series. Dashed lines are for correlations which are not causations, and bold arrows correspond to conditioning variables.

Definition 5. The conditional causal temporal mutual information between two time series $X^{(p)}$ and $X^{(q)}$ conditioned on a set $X^{(R)} = \{X^{(r_1)}, \dots, X^{(r_K)}\}$ is given by:

$$\begin{aligned} &CTMI(X^{(p)}; X^{(q)} \mid X^{(R)}) \\ &= I(X_t^{(p; \bar{\lambda}_{pq})}; X_{t+\tilde{\gamma}_{pq}}^{(q; \bar{\lambda}_{qp})} \mid (X_{t-\bar{\Gamma}_k}^{(r_k; \bar{\lambda}_k)})_{1 \leq k \leq K}, X_{t-1}^{(p; 1)}, X_{t+\tilde{\gamma}_{pq}-1}^{(q; 1)}), \end{aligned} \quad (2)$$

where $(\bar{\Gamma}_1, \dots, \bar{\Gamma}_K)$ and $(\bar{\lambda}_1, \dots, \bar{\lambda}_K)$ correspond to the optimal conditional gaps and window sizes which minimize, for $\bar{\Gamma}_1, \dots, \bar{\Gamma}_K \geq \max(1, \text{sgn}(\tilde{\gamma}_{pq})|\tilde{\gamma}_{pq} + 1|)$:

$$I \left(X_t^{(p; \bar{\lambda}_{pq})}; X_{t+\tilde{\gamma}_{pq}}^{(q; \bar{\lambda}_{qp})} \mid (X_{t-\bar{\Gamma}_k}^{(r_k; \bar{\lambda}_k)})_{1 \leq k \leq K}, X_{t-1}^{(p; 1)}, X_{t+\tilde{\gamma}_{pq}-1}^{(q; 1)} \right).$$

By considering the minimum over compatible lags and window sizes, one guarantees that if there exist conditioning variables which make the two time series independent, they will be found.

Figure 3 illustrates the above on two different examples. On the left, $X_{t-1}^{(p)}$ is correlated to $X_t^{(q)}$ as $X_{t-2}^{(r)}$ is a common cause with a lag of 1 for $X^{(p)}$ and a lag of 2 for $X^{(q)}$. Conditioning on $X_{t-2}^{(r)}$ removes the dependency between $X^{(p)}$ and $X^{(q)}$. Note that all time series have here a window of size 1. On the right, $X^{(r_1)}$ and $X^{(r_2)}$ are common causes of $X^{(p)}$ and $X^{(q)}$: $X^{(r_1)}$ causes $X^{(p)}$ and $X^{(q)}$ with temporal lag of 1, which renders $X^{(p)}$ and $X^{(q)}$ correlated at the same time point, while $X^{(r_2)}$ causes $X^{(p)}$ and $X^{(q)}$ with temporal lag of 1 and 2 respectively, which renders $X^{(p)}$ and $X^{(q)}$ correlated at lagged time points. The overall correlation between $X^{(p)}$ and $X^{(q)}$ is captured by considering a window size of 2 in $X^{(q)}$. All other time series have a window size of 1. By conditioning on both $X^{(r_1)}$ and $X^{(r_2)}$, $X^{(p)}$ and $X^{(q)}$ become independent.

Estimation As in Runge [2018], we rely on the k -nearest neighbor method for the estimation of CTMI. The distance between two windows considered here is

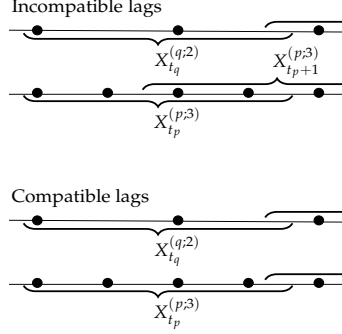


Figure 4: Illustration for constructing sequences of windows for two time series with different sampling rates.

the supremum distance, *i.e.* the maximum of the absolute difference between any two values in the two windows.

3.4 Extension to time series with different sampling rates

The above development readily applies to time series with different sampling rates as one can define window-based representations of the two time series as well as a sequence of joint observations.

Indeed, as one can note, Def. 1 does not rely on the fact that the time series have the same sampling rates. Figure 4 displays two time series $X^{(p)}$ and $X^{(q)}$ with different sampling rates where, while $\lambda_{pq} = 2$ and $\lambda_{qp} = 3$, the time spanned by each window is the same. The joint sequence of observations, relating pairs of windows from $X^{(p)}$ and $X^{(q)}$ in the form $S = \{(w_{1_p}^{(p;\lambda_{pq})}, w_{1_q}^{(q;\lambda_{qp})}), \dots, (w_{n_p}^{(p;\lambda_{pq})}, w_{n_q}^{(q;\lambda_{qp})})\}$, should however be such that for all index i of the sequence one has: $s(w_{i_q}^{(q;\lambda_{qp})}) = s(w_{i_p}^{(p;\lambda_{pq})}) + \gamma_{pq}$, where $s(w)$ represents the starting time of the window w , and γ_{pq} is constant over time. This is not the case for the first example, but is true for the second one, which is a relevant sequence of observations.

If the two time series are sufficiently long, there always exists a correct sequence of joint observations. Indeed, if the window sizes λ_{pq} and λ_{qp} are known, let $\gamma_{pq} = s(w_1^{(q;\lambda_{qp})}) - s(w_1^{(p;\lambda_{pq})})$. Furthermore, let τ_p and τ_q denote the number of observations per time unit³. Then, λ_{pq} , λ_{qp} and γ_{pq} are compatible through the set of joint observations S with $s(w_{i_p}^{(p;\lambda_{pq})}) = s(w_1^{(p;\lambda_{pq})}) +$

³Time unit corresponds to the largest (integer) time interval according to the sampling rates of the different time series. For example, if a time series has a sampling rate of 10 per second and another a sampling rate of 3 per 10 minutes, then the time unit is equal to 10 minutes.

$(i_p - 1)LCM(\tau_p, \tau_q)$ and $s(w_{i_q}^{(q;\lambda_{qp})}) = s(w_1^{(q;\lambda_{qp})}) + (i_q - 1)LCM(\tau_p, \tau_q)$, with LCM the lowest common multiple.

4 PCTMI: a Causal discovery algorithm for Time Series

We present in this section a new method for causal discovery in time series based on the causal temporal mutual information introduced above to construct the skeleton of the causal graph. This skeleton is then oriented on the basis of the Entropy Reduction Principle and the PC algorithm. Our method assumes both the Causal Markov Condition and Faithfulness of the data distribution, which are classical assumptions for causal discovery within constraint-based methods.

4.1 Skeleton construction

We follow the same steps as the ones of the PC algorithm [Spirtes et al., 2000] which assumes that all variables are observed. It aims at building causal graphs by orienting a skeleton obtained, from a complete graph, by removing edges connecting independent variables. The causal summary graphs considered are directed acyclic graphs (DAG) in which self-loops are allowed to represent temporal dependencies within a time series. In the remainder of the paper, we assess whether the scores provided by CTMI are small enough for the time series to be considered independent through a permutation test, following Runge [2018].

Starting with a complete graph that relates all time series, the first step consists in computing CTMI for all pairs of time series and removing edges if the two time series are considered independent. Once this is done, one checks, for the remaining edges, whether the two time series are conditionally independent (the edge is removed) or not (the edge is kept). Starting from a single time series connected to $X^{(p)}$ or $X^{(q)}$, the set of conditioning time series is gradually increased till either the edge between $X^{(p)}$ and $X^{(q)}$ is removed or all time series connected to $X^{(p)}$ and $X^{(q)}$ have been considered. We will denote by $\text{sepset}(p, q)$ the separation set of $X^{(p)}$ and $X^{(q)}$, which corresponds to the smallest set of time series connected to $X^{(p)}$ and $X^{(q)}$ such that $X^{(p)}$ and $X^{(q)}$ are conditionally independent given this set. Note that we make use of the same strategy as the one used in PC-stable [Colombo and Maathuis, 2014], which consists in sorting time series according to their CTMI scores and, when an independence is detected, removing all other occurrences of the time series. This leads to an order-independent procedure.

The following theorem states that the skeleton obtained by the above procedure is the true one.

Theorem 1. Let $\mathcal{G} = (V, E)$ be a summary graph, and assume that we are given perfect conditional independence information about all pairs of variables $(X^{(p)}, X^{(q)})$ in V given subsets $S \subseteq V \setminus \{X^{(p)}, X^{(q)}\}$. Then the skeleton previously constructed is the skeleton of \mathcal{G} .

Proof. Let us consider two time series $X^{(p)}$ and $X^{(q)}$. If they are independent, then $\text{CTMI}(X^{(p)}; X^{(q)}) = 0$ as one considers the maximum over window sizes and lags in CTMI, and so by the causal Markov condition and faithfulness, there is no edge between $X^{(p)}$ and $X^{(q)}$ in the corresponding skeleton, as in the true one. If however they are dependent or independent conditioned on other time series, then the windows of $X^{(p)}$ and $X^{(q)}$ contain the true related instants (otherwise CTMI would not be maximum since we are given perfect conditional independence information) and so variables $X^{(p)}$ and $X^{(q)}$ are adjacent in \mathcal{G} by the causal Markov condition and faithfulness. As we follow the PC algorithm, we test all necessary conditioning sets to ensure that we remove unnecessary edges. The notion of window introduced in CTMI allows to consider all the relevant instants, and the chaining rule removes unnecessary instants within the window. \square

4.2 Orientation

Once the skeleton has been constructed, one tries to orient as many edges as possible. To do so, we first notice here that Theorem 1 entails that each edge in the skeleton, which is associated with a *prima facie* cause, corresponds to a true causal relation, the orientation of which is provided by the direction of the *prima facie* cause, *i.e.*:

Corollary 1. By Property 1, every edge in the skeleton obtained by the above procedure corresponds to a *prima facie* cause and by, causal sufficiency, to a true causal relation between the related time series. Furthermore, the orientation of this causal direction is directly given by the orientation of the *prima facie* cause.

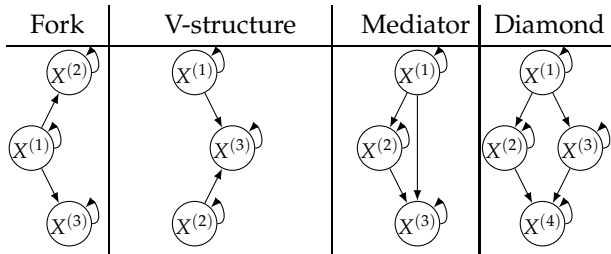
Corollary 1 allows us to introduce a new orientation rule, given below.

ER-Rule 0 (Entropy Reduction - γ). In a pair $X^{(p)} - X^{(q)}$, if $\tilde{\gamma}_{pq} > 0$, then orient the edge as: $X^{(p)} \rightarrow X^{(q)}$.

Proof. For a pair $X^{(p)} - X^{(q)}$ in the skeleton, if $\tilde{\gamma}_{pq} > 0$, then, by Def. 4, $X^{(p)}$ is an entropic *prima facie* cause of $X^{(q)}$ and by Corollary 1 the edge should be oriented from $X^{(p)}$ to $X^{(q)}$. \square

Furthermore, we make use of the following heuristic rule to orient additional edges when the optimal gap $\tilde{\gamma}_{pq}$ is null. This heuristic is based on the intuition that the difference in the window sizes is, when the optimal lag is null, an indication of the direction of the causal relation when there are common causes with different lags for the two time series under consideration.

Table 1: Structures of simulated data.



ER-Rule 1 (Entropy Reduction - λ). In a pair $X^{(p)} - X^{(q)}$, if $\bar{\gamma}_{pq} = 0$, $\bar{\lambda}_{pq} < \bar{\lambda}_{qp}$ and for all $X^{(r)}$ s.t. $X^{(q)} \leftarrow X^{(r)} \rightarrow X^{(p)}$, $\bar{\gamma}_{rp}, \bar{\gamma}_{rq} < \bar{\lambda}_{pq}$, then orient the edge as: $X^{(p)} \rightarrow X^{(q)}$.

Once all possible edges have been oriented using the above two rules, we apply the orientation rules of the PC algorithm⁴, using the standard mutual information with lags equal to 0 and window sizes to 1 as the only edges not oriented with the above rules have a lag of 0 and equal window sizes. Algorithm 1 summarizes the steps used to construct the causal graph (a detailed algorithm is given in Appendices). We refer to the overall process as PCTMI.

Algorithm 1 PCTMI

Require: \mathcal{X} a d -dimensional time series

1. Construction of the skeleton using CTMI
2. Orient as many edges as possible using **ER-Rules**
3. Apply orientation rules of PC: (a) orient edges with the origin of causality, then (b) recursively orient new edges with the other rules

Return the summary graph \mathcal{G}

5 Experiments

To illustrate the behavior of our method⁵, we rely on both artificial and real-world datasets as well as several state-of-the-art methods.

Datasets The artificial datasets⁶ correspond to four different causal structures (fork, V-structure, mediator, diamond) presented in Table 1. The data generat-

⁴These rules are given in Appendices.

⁵Code available in the Supplementary Material

⁶Available in the Supplementary Material

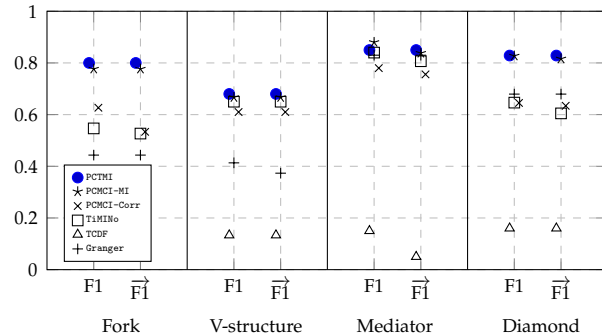


Figure 5: Performance for the summary graph inference for 4 toy structures. We report the mean for F1 score, about the non oriented and the oriented graph.

ing process is the following: for all q , for all $t > 0$,

$$X_t^{(q)} = a_{t-1}^{qq} X_{t-1}^{(q)} + \sum_p a_{t-\gamma}^{pq} f(X_{t-\gamma}^{(p)}) + 0.1 \zeta_t^q,$$

where $\gamma \geq 0$, $a_t^{jq} \sim \mathcal{U}([-1; -0.1] \cup [0.1; 1])$ for all $1 \leq j \leq d$, $\zeta_t^q \sim \mathcal{N}(0, \sqrt{15})$ and f is a non linear function chosen at random in {absolute value, tanh, sine, cosine}. Datasets corresponding to those structures are available with both equal and different sampling rates.

The real-world dataset is the benchmark of FMRI (Functional Magnetic Resonance Imaging) data that contains BOLD (Blood-oxygen-level dependent) datasets for 28 different underlying brain networks⁷ [Smith et al., 2011]. BOLD FMRI measures the neural activity of different regions of interest in the brain based on the change of blood flow. There are 50 regions in total, each with its own associated time series. Since not all existing methods can handle 50 time series, datasets with more than 10 time series are excluded.

In all different experimental settings, we compare the results of different algorithms using two different measures, the *F1-score* (F1) of the adjacencies (without self causes, as there are assumed to be true with lag 1) in the graph obtained and its oriented version ($\vec{F1}$).

Experimental setup For comparison purposes, we consider, in addition to the proposed PCTMI, five state-of-the-art methods. PCMCI-MI and PCMCI-Corr are both derived from PCMCI, a constraint-based method introduced in Runge et al. [2019], in which the former is based on the mutual information independence test whereas the latter is based on a linear partial correlation independence test. For both methods we used the authors’ implementation from the Python Tigramite module⁸. TiMINo is a Structural Equation Model method introduced

⁷Original data: <https://www.fmrib.ox.ac.uk/datasets/netstim/index.html>
Preprocessed version: <https://github.com/M-Nauta/TCDF/tree/master/data/fMRI>
⁸<https://github.com/jakobrunge/tigramite>

Table 2: Performance for the summary graph inference for the FMRI benchmark. We report the mean and the standard deviation for the two measures.

	PCTMI	PCMCI-MI	PCMCI-Corr	TiMINo	TCDF	Granger
F1	0.67 \pm 0.20	0.38 \pm 0.23	0.45 \pm 0.22	0.56 \pm 0.21	0.13 \pm 0.20	0.56 \pm 0.18
$\vec{F1}$	0.44 \pm 0.26	0.22 \pm 0.19	0.29 \pm 0.20	0.32 \pm 0.11	0.07 \pm 0.12	0.24 \pm 0.17

in Peters et al. [2013]. We used the code available in R⁹ and assumed a linear time series model since only this model was fully implemented by the authors. TCDF is a Neural Network based method introduced in Nauta et al. [2019]. We used the code available on the authors’ website¹⁰. To train the Neural Network, we relied on the default hyperparameters presented in the original paper (Mean Squared Error as loss function, Adam optimization algorithm with 5000 of epochs, learning rate equals to 0.01, dilation coefficient equals to 4 and kernel size equals to 4, 1 hidden layer). The last method is Granger [Granger, 2004], for which we use the multivariate version which compares the full model with the restricted model (which removes one of the variables) to assess whether the absence of that variable will decrease the accuracy significantly. For TiMINO and Granger, the best time lag is determined with the Akaike Information Criterion.

The window sizes and lags are limited to 5. The test level is set to $\alpha = 0.05$. Lastly, some methods are meant to build a full temporal graph (PCMCI and TCDF). To obtain the summary graph inferred by these methods, we simply consider that if there exists at least one node $X_t^{(p)}$ that causes a node $X_{t'}^{(q)}$ in the full temporal graph for some time points t and t' , then $X^{(p)}$ causes $X^{(q)}$ in the summary graph.

Results The results for the simulations are summarized in Figure 5. Note that standard deviations are not displayed for sake of clarity, with similar values between the best methods (the complete results are given in Appendices). As one can note, our proposed algorithm consistently outperforms all other methods. Furthermore, the similarity of results obtained by the F1 and $\vec{F1}$ scores illustrates the stability of our method.

When comparing the overall performance on the FMRI benchmark (Ta-

⁹<http://web.math.ku.dk/~peters/code.html>

¹⁰<https://github.com/M-Nauta/TCDF>

Table 3: Results obtained by PCTMI with different sampling rates on the 4 structures. We report the mean and the standard deviation for the two measures.

	Fork	V-structure	Mediator	Diamond
F1	0.83 \pm 0.31	0.4 \pm 0.32	0.88 \pm 0.09	0.79 \pm 0.09
$\vec{F1}$	0.78 \pm 0.31	0.27 \pm 0.32	0.88 \pm 0.09	0.44 \pm 0.16

ble 2), PCTMI clearly outperforms other methods in inferring the skeleton as well as in orientation, despite the fact that there exist short time series in FMRI. All other methods are comparable, except TCDF which performs very poorly. Interestingly, PCMCI-Corr performs better than PCMCI-MI, which suggests the existence of linear causal relations.

We also assessed the behavior of PCTMI when the time series have different sampling rates. The results are presented in Table 3. As one can see, its performance is close to the ones obtained with equal sampling rates, the degradation being not really surprising as one has less data to rely on.

Lastly, we show in Appendices that PCTMI is of lower complexity and empirically faster than PCMCI-MI, which is overall the closest competitor to our approach.

6 Conclusion

We have addressed in this study the problem of learning a summary causal graph on time series with equal or different sampling rates. To do so, we have first proposed a new temporal mutual information measure defined on a window-based representation of time series. We have then showed how this measure relates to an Entropy Reduction Principle that can be seen as a special case of the Probabilistic Raising Principle. We have finally combined these two ingredients in a PC-like algorithm to construct the summary causal graph. Experiments conducted on different benchmark datasets, including equal and different sampling rates, show both the efficacy and efficiency of our approach.

References

- Séverine Affeldt and Hervé Isambert. Robust reconstruction of causal graphical models based on conditional 2-point and 3-point information. In *Proceedings of the Thirty-First Conference on Uncertainty in Artificial Intelligence, UAI'15*, 2015. ISBN 978-0-9966431-0-8.
- David J. Albers and George Hripcsak. Estimation of time-delayed mutual information and bias for irregularly and sparsely sampled time-series. *Chaos, Solitons & Fractals*, 45(6):853 – 860, 2012.
- Tianjiao Chu and Clark Glymour. Search for additive nonlinear time series causal models. *Journal of Machine Learning Research*, 9:967–991, 2008.
- Diego Colombo and Marloes H. Maathuis. Order-independent constraint-based causal structure learning. *Journal of Machine Learning Research*, 15(116): 3921–3962, 2014.
- Doris Entner and Patrik Hoyer. On causal discovery from time series data using fci. *Proceedings of the 5th European Workshop on Probabilistic Graphical Models, PGM 2010*, 2010.

- Stefan Frenzel and Bernd Pompe. Partial mutual information for coupling analysis of multivariate time series. *Physical review letters*, 99:204101, 2007.
- Andreas Galka, Tohru Ozaki, Jorge Bosch Bayard, and Okito Yamashita. Whitening as a tool for estimating mutual information in spatiotemporal data sets. *Journal of Statistical Physics*, 124(5):1275–1315, 2006.
- Clive Granger. Investigating causal relations by econometric models and cross-spectral methods. *Econometrica*, 37(3):424–38, 1969.
- Clive W. J. Granger. Time series analysis, cointegration, and applications. *The American Economic Review*, 94(3):421–425, 2004. ISSN 00028282.
- Aapo Hyvärinen, Shohei Shimizu, and Patrik O. Hoyer. Causal modelling combining instantaneous and lagged effects: An identifiable model based on non-gaussianity. In *Proceedings of the 25th International Conference on Machine Learning, ICML '08*, pages 424–431, New York, NY, USA, 2008. ACM. ISBN 978-1-60558-205-4.
- Aapo Hyvärinen, Kun Zhang, Shohei Shimizu, and Patrik O. Hoyer. Estimation of a structural vector autoregression model using non-gaussianity. *J. Mach. Learn. Res.*, 11:1709–1731, 2010. ISSN 1532-4435.
- Alexander Kraskov, Harald Stögbauer, and Peter Grassberger. Estimating mutual information. *Physical review. E, Statistical, nonlinear, and soft matter physics*, 69 6 Pt 2:066138, 2004.
- Daniel Malinsky and David Danks. Causal discovery algorithms: A practical guide. *Philosophy Compass*, 13(1), 2018.
- Daniel Malinsky and Peter Spirtes. Causal structure learning from multivariate time series in settings with unmeasured confounding. In *Proceedings of 2018 ACM SIGKDD Workshop on Causal Discovery*, volume 92 of *Proceedings of Machine Learning Research*, pages 23–47, London, UK, 2018. PMLR.
- Alessio Moneta, Doris Entner, Patrik O. Hoyer, and Alex Coad. Causal inference by independent component analysis: Theory and applications. *Oxford Bulletin of Economics and Statistics*, 75(5):705–730, 2013.
- Meike Nauta, Doina Bucur, and Christin Seifert. Causal discovery with attention-based convolutional neural networks. *Machine Learning and Knowledge Extraction*, 1(1):312–340, 1 2019. ISSN 2504-4990.
- Jonas Peters, Dominik Janzing, and Bernhard Schölkopf. Causal inference on time series using restricted structural equation models. In *Advances in Neural Information Processing Systems 26*, pages 154–162, 2013.
- Jakob Runge. Conditional independence testing based on a nearest-neighbor estimator of conditional mutual information. In Amos Storkey and Fernando Perez-Cruz, editors, *Proceedings of the Twenty-First International Conference on*

Artificial Intelligence and Statistics, volume 84 of *Proceedings of Machine Learning Research*, pages 938–947, Playa Blanca, Lanzarote, Canary Islands, 09–11 Apr 2018. PMLR.

Jakob Runge, Peer Nowack, Marlene Kretschmer, Seth Flaxman, and Dino Sejdinovic. Detecting and quantifying causal associations in large nonlinear time series datasets. *Science Advances*, 5(11), 2019.

Thomas Schreiber. Measuring information transfer. *Physical review letters*, 85: 461–4, 2000.

Claude Elwood Shannon. A mathematical theory of communication. *The Bell System Technical Journal*, 27(3):379–423, 1948.

Stephen M. Smith, Karla L. Miller, Gholamreza Salimi Khorshidi, Matthew A. Webster, Christian F. Beckmann, Thomas E. Nichols, Joseph Ramsey, and Mark W. Woolrich. Network modelling methods for fmri. *NeuroImage*, 54: 875–891, 2011.

Peter Spirtes, Clark Glymour, and Richard Scheines. *Causation, Prediction, and Search*. MIT press, 2nd edition, 2000.

Patrick Suppes. *A Probabilistic Theory of Causality*. Amsterdam: North-Holland Pub. Co., 1970.

A Algorithm

The pseudo-code of PCTMI is presented below. $\text{Adj}(X^{(q)}, \mathcal{G})$ represents all adjacent nodes to $X^{(q)}$ in the graph \mathcal{G} and $\text{sepset}(p, q)$ is the separation set of $X^{(p)}$ and $X^{(q)}$.

Algorithm 2 PCTMI

Require: X a d -dimensional time series of length T , $\tau_{\max} \in \mathbb{N}$ the maximum number of lags, α a significance threshold
Form a complete undirected graph $\mathcal{G} = (V, E)$ with d nodes
 $n = 0$
while there exists $X^{(q)} \in V$ such that $\text{card}(\text{Adj}(X^{(q)}, \mathcal{G})) \geq n + 1$ **do**
 $\mathbf{D} = \text{list}()$
 for $X^{(q)} \in V$ s.t. $\text{card}(\text{Adj}(X^{(q)}, \mathcal{G})) \geq n + 1$ **do**
 for $X^{(p)} \in \text{Adj}(X^{(q)}, \mathcal{G})$ **do**
 for all subsets $X^{(\mathbf{R})} \subset \text{Adj}(X^{(q)}, \mathcal{G}) \setminus \{X^{(p)}\}$ such that $\text{card}(X^{(\mathbf{R})}) = n$
 and $(\gamma_{rp} \geq 0$ or $\gamma_{rq} \geq 0)$ for all $r \in \mathbf{R}$ **do**
 $y_{q,p,\mathbf{R}} = \text{CTMI}(X^{(p)}; X^{(q)} \mid X^{(\mathbf{R})})$
 $\text{append}(\mathbf{D}, \{X^{(q)}, X^{(p)}, X^{(\mathbf{R})}, y_{q,p,\mathbf{R}}\})$
 end for
 end for
 end for
Sort \mathbf{D} by increasing order of y
while \mathbf{D} is not empty **do**
 $\{X^{(q)}, X^{(p)}, X^{(\mathbf{R})}, y\} = \text{pop}(\mathbf{D})$
 if $X^{(p)} \in \text{Adj}(X^{(q)}, \mathcal{G})$ and $X^{(\mathbf{R})} \subset \text{Adj}(X^{(q)}, \mathcal{G})$ **then**
 if test $\text{CTMI}(X^{(p)}; X^{(q)} \mid X^{(\mathbf{R})}) > \alpha$ **then**
 Remove edge $X^{(p)} - X^{(q)}$ from \mathcal{G}
 $\text{sepset}(p, q) = \text{sepset}(q, p) = X^{(\mathbf{R})}$
 end if
 end if
end while
 $n = n + 1$
end while
for each connected pair in \mathcal{G} **do** apply ER-Rules.
for each triple in \mathcal{G} **do** apply PC-Rule 0
while no more edges can be oriented **do**
 for each triple in \mathcal{G} **do** apply PC-Rules 1, 2, 3
end while
Return the summary graph \mathcal{G}

B PC Rules

We recall in this section orientation rules of the PC algorithm.

PC-Rule 0 (Origin of causality). *In an unshielded triple $X^{(p)} - X^{(r)} - X^{(q)}$ such that $X^{(r)} \notin \text{sepset}(p, q)$, if $I(X_t^{(p)}; X_t^{(q)} | X_t^{(r)}, \text{sepset}(p, q)) > 0$, then $X^{(r)}$ is an unshielded collider: $X^{(p)} \rightarrow X^{(r)} \leftarrow X^{(q)}$.*

PC-Rule 1 (Propagation of causality). *In an unshielded triple $X^{(p)} \rightarrow X^{(r)} - X^{(q)}$, if $X^{(r)} \in \text{sepset}(p, q)$ then orient the unshielded triple as $X^{(p)} \rightarrow X^{(r)} \rightarrow X^{(q)}$.*

PC-Rule 2. *If there exist a direct path from $X^{(p)}$ to $X^{(q)}$ and an edge between $X^{(p)}$ and $X^{(q)}$, then orient $X^{(p)} \rightarrow X^{(q)}$.*

PC-Rule 3. *If there exists an unshielded triple $X^{(p)} \rightarrow X^{(r)} \leftarrow X^{(q)}$ and an unshielded triple $X^{(p)} - X^{(s)} - X^{(q)}$, then orient $X^{(s)} \rightarrow X^{(r)}$.*

C Complexity analysis

Our proposed method benefits from a smaller number of tests compared to constraint-based methods that infer the full temporal graph. In the worst case, the complexity of PC in a temporal graph is bounded by:

$$\frac{(d \cdot \tau_{max})^2 (d \cdot \tau_{max} - 1)^{k-1}}{(k-1)!},$$

where k represents the maximal degree of any vertex and τ_{max} is the maximum number of lags. Each operation consists in conducting a significance test on a conditional independence measure. Algorithms adapted to time series, as PCMCI [Runge et al., 2019], rely on time information to reduce the number of tests. Indeed, with this information, the complexity can be divided by 2 (when instantaneous relations are not taken into account). PCTMI infers a summary graph, which limits the number of decisions that need to be taken. Indeed,

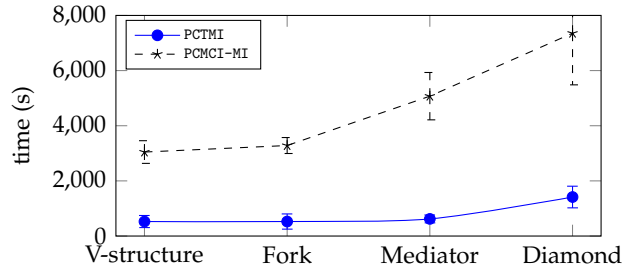


Figure 6: Time computation (in seconds) for PCTMI and PCMCI-MI.

PCTMI's complexity in the worst case (when all relations are instantaneous) is bounded by:

$$\frac{d^2(d-1)^{k-1}}{(k-1)!}.$$

Figure 6 provides an empirical illustration of the difference in complexity of the two approaches on the four structures (v-structure, fork, mediator, diamond), sorted according to their number of nodes, their maximal out-degree and their maximal in-degree. The time is given in seconds. As one can note, PCTMI is always faster than PCMI-MI, the difference being more important when the structure to be inferred is complex.